Journal of Applied Polymer Science

Exploring the Role of Stearic Acid in Modified Zinc Aluminum Layered Double Hydroxides and Their Acrylonitrile Butadiene Rubber Nanocomposites

Subramani Bhagavatheswaran Eshwaran,[1,2] Debdipta Basu,[1,2] Sankar Raman Vaikuntam,[1,2] Burak Kutlu,[1,2] Sven Wiessner,[1,2] Amit Das,[1] Kinsuk Naskar,[3] Gert Heinrich[1,2]

[1]Leibniz-Institut für Polymerforschung Dresden e.V., Hohe Strasse 6, D-01069 Dresden, Germany
[2]Technische Universität Dresden, Institut für Werkstoffwissenschaft, D-01062 Dresden, Germany
[3]Rubber Technology Centre, Indian Institute of Technology Kharagpur, Kharagpur, India
Correspondence to: S. Wiessner (E-mail: wiessner@ipfdd.de)

ABSTRACT: The proposed study attempted to explore the role of stearic acid modification on the properties of zinc-aluminum based layered double hydroxides (LDH) and their composites with acrylonitrile butadiene rubber (NBR). Three distinctive LDH systems were adapted for such comparison; an unmodified LDH and two stearic acid modified LDH. The use of zinc oxide and stearic acid in the rubber formulation was avoided as the modified LDH would be able to deliver the necessary activators for the vulcanization process. Emphasis was predominantly given to reconnoiter the merits of stearic acid modification on the increase in interlayer distance of the LDH. X-ray diffraction studies and transmission electron microscope morphological investigations of LDH powders indicated that modification with stearic acid increased the interlayer spacing which would favor the intercalation of NBR polymer chains into the layered space. However, stress–strain studies indicated better mechanical properties for composites with unmodified LDH. Composites with LDH showed higher crosslinking densities than conventionally sulfur cured control compounds using zinc oxide/stearic acid as activators. This was evident from equilibrium swelling method as well as statistical theory of rubber elasticity. © 2014 Wiley Periodicals, Inc. J. Appl. Polym. Sci. **2015**, *132*, 41539.

KEYWORDS: crosslinking; elastomers; mechanical properties; properties and characterization; rubber

Received 18 June 2014; accepted 19 September 2014
DOI: 10.1002/app.41539

INTRODUCTION

Fillers with particle sizes in the nanometer range like layered silicate, montmorillonite, carbon nanotubes, graphene, layered double hydroxide (LDH) etc. are gaining interest recently as suitable fillers for rubbers because of their excellent reinforcing capabilities.[1–4] Simultaneously, efforts are also been given to materials which can serve as multifunctional additives (MFA) in the field of rubber technology.[4,5] MFA are ingredients added into the rubber formulation with the capability of performing more than one intended task. On the other hand, constant efforts are also being laid focusing toward replacement or reduction of the amount of zinc oxide in rubber formulations, due to certain toxicity of zinc on the aquatic life.[6] As an outcome many substituents have emerged with potentials equivalent to zinc oxide.[3,5–11] LDH based on zinc and aluminum is one such material that qualifies itself as MFA, having the ability to replace zinc oxide in rubbers[3,10] and also participating in mechanical reinforcement of the rubber matrix. Research works on rubber LDH composites are ample, yet the treatment of LDH as a MFA is not very much looked upon.[12–16]

LDH are generally denoted in the empirical form as $[M^{II}_{1-x}M^{III}_{x}(OH)_2]^{x+}[A^{n-}]_{x/n}\cdot yH_2O$, where the anions A^{n-} occupy the interlayer and are sandwiched in-between the M^{II} and M^{III} divalent and trivalent metal cationic layers.[17–21] Tailoring the properties of LDH can be done in two different ways where the first route involves modification of chemical composition and/or the structure of naturally occurring Mg-Al-LDH (hydrotalcite) by various techniques[9,22] and the other is by synthesizing the desired LDH adapting different experimental methods.[19,23,24] Moreover, the organophilic modification of LDH is also essential to disperse LDH in nonpolar polymers, as LDH is polar in nature due to the presence of number of hydroxyl groups in its structure. Figure 1 depicts the structures of LDH in (a) its unmodified form with less interlayer distance and (b) after modification with stearic acid which leads to stearate ions present in the interlayer resulting in increased interlayer distance, facilitating high intercalation of polymeric chains.

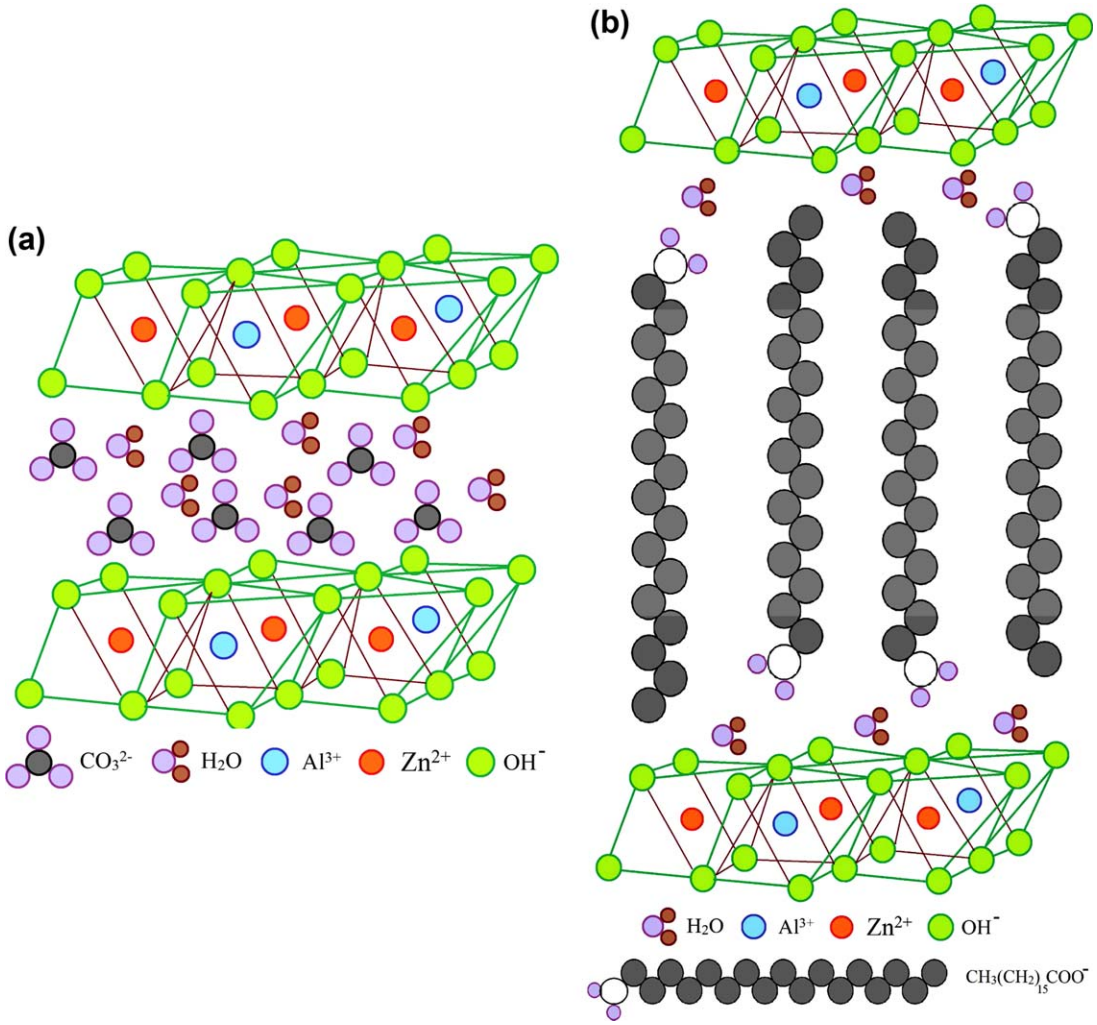

Figure 1. Schematic representation of (a) unmodified Zn-Al LDH, (b) Stearate ion modified Zn-Al LDH. [Color figure can be viewed in the online issue, which is available at wileyonlinelibrary.com.]

In our previous works,[3,25] it was proved that Zn-Al LDH has the potential to replace zinc oxide in a typical rubber formulation and additionally possess the ability to impart reinforcement to the rubber matrix. However, it is well known that during vulcanization conditions (at higher temperature and pressure), ZnO along with stearic acid reacts with sulfur and organic accelerators resulting into a soluble sulfurating complex.[26] Therefore, it would be an interesting task to observe how the crystal layers of stearate modified Zn-Al LDH interacts with the curing ingredients and their ability to contribute toward the mechanical reinforcement as layered mineral fillers[1] inside the rubber matrix. In an attempt to fathom the advantages of stearate modification, acrylonitrile butadiene rubber (NBR) was chosen as the matrix and subsequently nanocomposites of NBR with unmodified LDH, commercial stearate modified Zn-Al LDH, and self-synthesized stearate modified Zn-Al LDH were prepared. Zn-Al-stearate LDH was synthesized in laboratory with increased interlayer distance adapting the procedures reported in literatures,[27,28] which would kindle the intercalation of polymeric chains. Henceforth, the main objective is to highlight the merits and demerits of stearate modification and also to investigate the influence of increased gallery space of LDH on the resulting mechanical, crosslinking, and dynamic properties of the nanocomposites.

EXPERIMENTAL

Raw Materials

NBR (Perbunan 1846F—acrylonitrile content ~18%, Mooney viscosity ~46) and tertiary butyl benzothiazole sulfineamide (TBBS) were procured from Lanxess Germany. Zinc oxide, stearic acid, sulfur, and sodium salt were purchased from Acros organics, Belgium. Zinc nitrate, aluminum nitrate, and sodium hydroxide which are necessary for the synthesis of LDH were purchased from Sigma Aldrich. The unmodified commercial LDH (uLDHc) was Alcamizer P93 of Kisuma Chemicals with a chemical formula of Mg_3ZnAl_2 $(OH)_{12}$ CO_3 $3H_2O$ (purity>99%). The stearate modified commercial LDH (mLDHc) was purchased from Prolabin & Tefarm s.r.l., Italy (purity>99%). A stearate modified Zn-Al LDH (mLDHs) was synthesized in our laboratory according to the procedure available in literatures.[27,28] The chemical formula of mLDHc and mLDHs is $Zn_2Al(OH)_6$ $(C_{18}H_{35}O_2).2H_2O$.

Table I. Compounding Recipe with Different Types of LDH

	uLDHc	mLDHc	mLDHs	ZnO eq.
NBR 1846		100		
uLDHc	5			
mLDHc		5		
mLDHs			5	
ZnO				1.6
St. Ac				2.8
Sulfur		1.5		
TBBS		0.8		

Formulation

Three different rubber compounds were formulated based on the nature of LDH. The formulations are summarized and given in Table I. A LDH free compound was prepared with 1.6 phr ZnO and 2.8 phr stearic acid which provides an equimolar concentration of zinc cations and stearate anions with respect to use of 5 phr of mLDHs instead.

Mixing Procedure and Curing

All the samples were compounded in a laboratory sized two roll mill, Polymix 110-L, size: 203 mm × 102 mm, Servitech GmbH, Wustermark, Germany. The compounds were prepared in two stages; Stage I with high temperature and higher shear rate to achieve good dispersion of the LDH into the matrix and Stage II mixing at low shear rate and lower temperature to incorporate the curatives. The rubber was first added onto the mill at 80°C and masticated for 2 min., followed by the addition and mixing of LDH at low friction ratio of 1 : 1.2 for 5 min after which the friction ratio was increased to 1 : 2 and mixed for 20 min. For second stage mixing, the mill was cooled to 40°C, and sulfur and TBBS were added and mixed for 6 min at a friction ratio of 1 : 1.2. The compounds were cured under pressure at 160°C up to their respective curing time (t_{90}) and the thickness of the vulcanized sample was about 2 mm.

Instruments and Methods

Rheometric study was done with a rubber process analyzer (RPA) (Scarabaeus V-50, Scarabaeus GmbH, Langgöns, Germany). The curing parameter "delta torque" is the difference between the highest torque (M_H) and the minimum torque (M_L) measured during the vulcanization tenure. Vulcanization time, or curing time, was calculated as the time to reach 90% of the ultimate torque ($M_H - M_L$). The thermo gravimetric analyses (TGA) of LDH powder was performed using TGA Q 5000 from TA instruments at a heating rate of 20 °C/min from room temperature to 800°C in nitrogen atmosphere with flow rate of 50 mL/min. Tensile tests were carried out with a universal testing machine (Zwick 1456, Z010, Ulm, Germany) with DIN 53504/S2/200 specification. The instrument was equipped with optical strain sensors and 1 kN load cell with constant test speeds of 200 mm/min. To measure the mechanical properties, three dumbbell shaped specimens were punched out from each rubber sample. The shore A hardness of 6 mm thick samples was measured using a Bareiss hardness tester with an indentation period of 3 s. For transmission electron microscope (TEM) analysis, ultra-thin sections of the rubber composites were cut by ultra-microtome at a temperature of about −80°C and images were captured using a Libra 200, Zeiss, TEM with an acceleration voltage of 200 kV. X-ray diffraction (XRD) measurements for powder LDH were carried out with a Philips XRD-6000 and/or with a Seifert XRD 3003 T/T at a wavelength of 1.542 Å (Cu-Ka radiation). The scanning 2θ angles ranged between 0.5° and 25° with a step-scanning rate of 2° min^{-1}. The visco-elastic properties of the rubber samples were characterized using a dynamic mechanical thermal analysis device (GABO-EPLEXOR 2000N) in tensile mode. The temperature sweep experiments was conducted within a temperature range of −60°C to +80°C, at 0.5% dynamic strain amplitude, 1% static strain, 10 Hz frequency, and heating rate of 2 °C/min. Strain sweep experiment was conducted at 20°C, within 0.2% to 30% dynamic strain, with a static strain of 60% and a frequency of 10 Hz. The degree of crosslinking was determined by equilibrium swelling method as well as Mooney–Rivlin theory. For equilibrium swelling studies, two different sets of samples were used to evaluate the crosslink density. First set of samples (pre-swollen samples) were subjected to solvent extraction by allowing them to swell in toluene for 72 h and subsequently drying at atmospheric conditions for 5 days. These dried samples were then subjected to swelling for 3 days in toluene and the swollen weights were used for analysis. The second sets of samples (fresh samples) were used without solvent extraction, they were allowed to swell in toluene for 3 days and the swollen weights were used for the calculation.

The equilibrium swelling is calculated using Flory–Rehner[29] equation

$$v_e = -\frac{\ln(1-v_r)+v_r+\chi_{12}.v_r^2}{V_s.(v_r^{1/3}-v_r/2)} \quad (1)$$

$$v_r = \frac{1/\rho_{sam}}{1/\rho_{sam} + Q/\rho_{sol}} \quad (2)$$

$$Q = (M_{sw}-M_i)/M_i \quad (3)$$

where, Q is the swelling ratio, M_i and M_{sw} are the mass of rubber before and after swelling, V_r is the volume fraction of the swollen polymer, ρ_{sam}, ρ_{sol} are the densities of rubber and solvent respectively (0.87 g/cc for toluene),[30] v_e is the cross-linking density of the polymer network, χ_{12} is the Flory–Huggins parameter (0.435 for NBR-Toluene),[30] V_s is the molar volume of swelling solvent (106.1 cc/mol for toluene).[30]

For Mooney–Rivlin studies, the fresh samples indicate specimens without any prior strain history (maturation time 24 h after vulcanization). The second set of samples were stretched up to 275% elongation and released to minimize the Mullins effect. This was performed for 10 times in a cyclic order and then finally stretched up to failure. A plot of reduced stress versus extension ratio was made and the slope and the intercept obtained by fitting a straight line were taken for further calculations.

$$\text{Reduced stress} = \frac{\sigma}{2(\lambda - 1/\lambda^2)} \quad (4)$$

$$\frac{\sigma}{2(\lambda - 1/\lambda^2)} = C_1 + C_2/\lambda \quad (5)$$

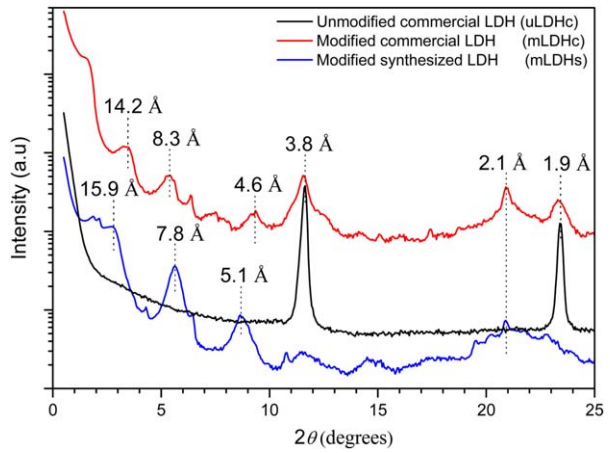

Figure 2. XRD plot for different types of (A) unmodified Zn-Al-LDH (u-LDH), (b) modified commercial Zn-Al-LDH (mLDHc), and (c) stearate ion modified Zn-Al LDH (mLDH). [Color figure can be viewed in the online issue, which is available at wileyonlinelibrary.com.]

$$\mathrm{CLD} = 1/M_c = C_1/RT \tag{6}$$

The Mooney–Rivlin theory is described as per eq. (5), σ is the stress, C_1 is the intercept, C_2 is the slope, λ is the extension ratio, M_c is the crosslink density or the inverse of molecular weight in between two successive crosslinks,[21,31] R is universal gas constant (8.314 J K^{-1} mol^{-1}) and T is room temperature (298 K).

RESULTS AND DISCUSSION

Characterization of LDH Filler

A typical diffractogram of LDH consists of sharp basal (001) reflections.[4,20,25] In Figure 2, uLDHc displays characteristic (003) LDH reflection at $2\theta = 11.6°$ and (006) reflection at $2\theta = 23.4°$ in the investigated range confirming the presence of hydrotalcite like structure[4,20,32] (LDH with carbonate interlayer ion). The first basal reflection (003) provides information about the interlayer distance of LDH, which is sum of the thickness of a single LDH layer and its gallery. Interlayer distance of uLDHc is found to be 0.38 nm according to Bragg's Law. The shift in the first LDH reflection is usually interpreted as intercalation of selected organic molecule into the LDH layers. This shift was observed for both mLDHs and mLDHc. However, the existence of clear pristine LDH relevant peaks ((003) and (006) planes) in mLDHc indicates that the intercalation or modification of stearate ions was not complete and it rather shows a mixed morphology with different space gaps between the two layers. mLDHs shows more prominent diffraction peaks and reflections of pristine LDH are almost totally absent indicating the success in synthesis compared to mLDHc. However, both mLDHc and mLDHs show a mixed morphology with different space gaps between the two layers explaining the multiple diffraction peaks at lower 2θ angles.

TEM studies are carried out with the powder LDH fillers and the micrographs are shown in Figure 3. It can be observed that uLDHc [Figure 3(a,b)] does not contain any fine laminar structure as the layers are much closer to one another. Whereas the modified LDH [Figure 3(c–f)] has precise and defined laminar structures indicating a very thin gap in between the two hydroxide crystal layers. The stearate ions used in the modification are present in between the layers and offering separation in between the layers. However, in both the modified materials some darker regions could be found which may arise due to the presence of unmodified LDH crystals or amorphous phase of the layered hydroxides. The study with TEM micrographs directly shows the crystalline structure of modified LDH with very small gap in between the layers and it also indicates a possibility to disperse or delaminate the crystal layers (exfoliation /intercalation) inside the rubber matrix.

Thermogravimetric analysis was carried out to understand the effect of organic modification on the thermal degradation behavior of the LDH. Figure 4 depicts the nature of weight loss and derivative weight against temperature. All the materials degrade in multiple steps and the first weight loss peak is observed below 100°C for mLDHs due to the presence of loosely bound surface water molecules. At nearly 160°C, a second weight loss was prominent in both the modified LDH and the most probable reason would be the evaporation of bound water molecules present in between the mineral layers and likewise for uLDHc this degradation step could be found at slightly higher temperature of 200°C. After losing entire water molecules, modified stearate group with decomposition temperature of ~350°C remains in the LDH and moreover it is evident that mLDHs undergoes a greater weight loss below 400°C indicating higher organic content (stearate content) than mLDHc. uLDHc leaves no trace of such peaks in this temperature region as there are no decomposable groups. Comparing mLDHc and mLDHs, it is clear that mLDHs contains higher amount of stearate functionality by virtue of the synthesis technique which could be attributed to the strong peak appearing at 400°C. The mLDHs has higher degradation stability than mLDHc as the peak is broader and is positioned at a slightly higher temperature. From the weight loss plot, it could be noted that uLDHc, mLDHc, and mLDHs have weight losses of 38%, 57%, and 69%, respectively. This indicates that mLDHc has a 50% more loss in weight with respect to uLDHc, and mLDHs has 82% more loss in weight with respect to uLDHc. This increment in loss in final weights in the filler is indirectly a representation of the amount of stearate modification.

Characterization of NBR/LDH Nanocomposites

The rheometric curing characteristics of the composites performed at 160°C for 60 min is shown in Table II. An astonishing observation is that the NBR composite filled with uLDHc (the LDH does not contain any stearate ions; it contains only zinc aluminum) was also being cured successfully. The cure rate index (CRI) was calculated using the expression $100/(T_{c90} - T_{s2})$ and NBR filled with mLDHs has the highest CRI of 15.7 min^{-1} which is 15% faster than uLDHc and 22% faster than mLDHc; a higher value of CRI represent faster vulcanization process. The faster cure of rubber compounds with mLDHs is materialized due to the effective formation of active zinc stearate coordination complex during vulcanization process which is aided by the excess stearate ions correlating with the results from TEM, XRD, and TGA. The maximum torque values of all the composites are incomparably near due to the lower loading of

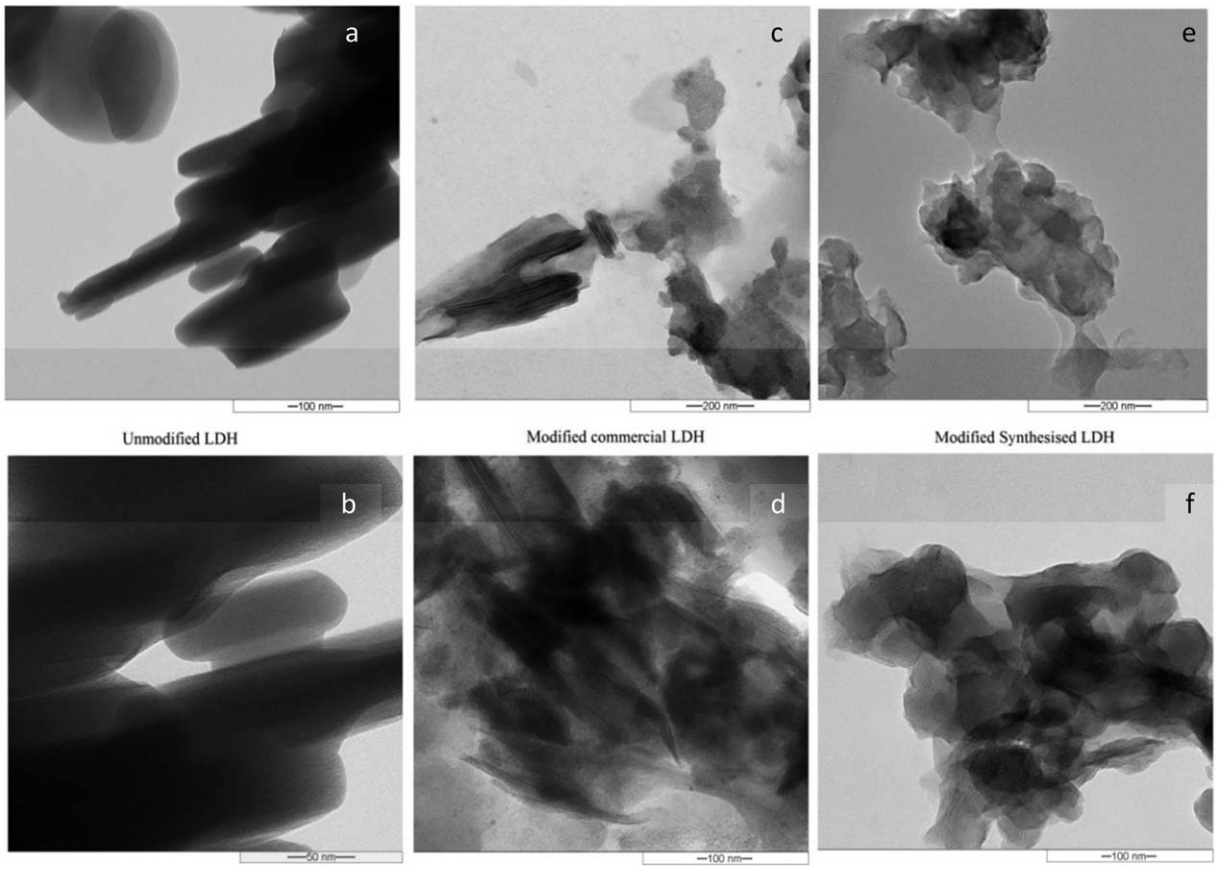

Figure 3. TEM images of different LDH: (a) uLDHc at 100 nm, (b) uLDHc at 50 nm, (c) mLDHc at 200 nm, (d) mLDHc at 100 nm, (e) mLDHs at 200 nm, (f) mLDHs at 100 nm.

the LDH. uLDHc has very less scorch time owing to the presence of hydroxyl groups on the surface of the fillers and also due to the lack of stearate ions. Therefore, finally it could be concluded that stearate modification in LDH helps to cure NBR matrix and also play a vital role in vulcanization kinetics of the NBR nanocomposites.

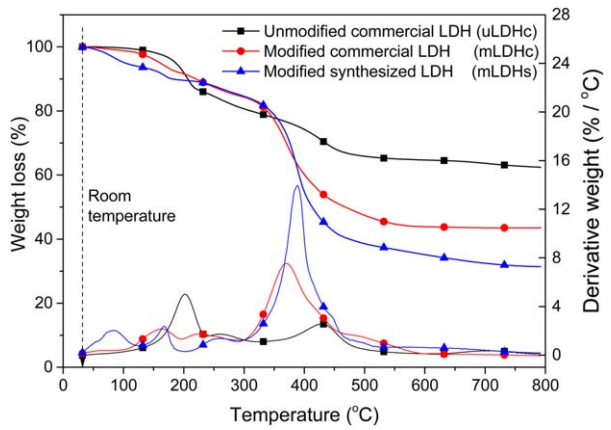

Figure 4. Weight loss and derivative weight vs. temperature plot for different powder LDH. [Color figure can be viewed in the online issue, which is available at wileyonlinelibrary.com.]

The uniaxial stress–strain properties and the shore A hardness data for NBR 1846 filled with three different types of LDH are given in Table III and Figure 6(a). The results indicate that stress values at 50% elongation of the unmodified and modified composites are equal, but as the strain increases there is a substantial difference in the stress values. The stress values of samples at 200% and 300% elongation exhibited by the uLDHc filled composite is ~23% and 41% higher mLDHc and mLDHs. uLDHc exhibits a maximum tensile strength of 4.7 MPa, which is 74% higher than mLDHc and 96% higher than mLDHs and also uLDHc has the maximum elongation at break of 495%. It is clear from XRD and TEM analysis that intercalation of polymer chains into the layers of modified LDH is easy but the reduction in the properties of both modified LDH composites could be due to the stearic acid modification, i.e. excessive amount of stearate groups leading to inferior properties as stearate groups tend to act as an internal lubricant.[33] From the TGA analysis, it is proved that mLDHs contains more stearate groups than mLDHc and this accounts for the inferior properties of the mLDHs filled nanocomposite. Also, from the vulcanization chemistry point of view there are possibilities of the layered structure of LDH getting collapsed due to the participation of the zinc and the stearate groups in the vulcanization reaction. It is assumed that the stearate modification will enhance the intercalation and facilitate better polymer–filler interaction, but the loss of reinforcing crystalline layers due to the formation of sulfurating complex is unforeseen.

Table II. Cure Characteristics of NBR 1846 Filled with 5 phr of Different LDH

	S′ Min (dN-m)	S′ Max (dN-m)	T_s 2 (min)	T_c 90 (min)	CRI Cure rate index (min^{-1})
uLDHc	0.60	6.07	4.41	11.83	13.48
mLDHc	0.60	6.21	8.10	16.26	12.25
mLDHs	0.59	6.07	6.84	13.21	15.70

The mechanical reinforcement offered by the crystalline layers must be enormous so as to overcome the lubricating effect of the stearate groups, whereas the above said reduction in the number of crystalline reinforcing structures that exist after the vulcanization reaction is certainly not ample to offer the expected mechanical strength to the matrix. Whereas mLDHc contains some proportion of unmodified crystal layers which was evident from the XRD and TEM micrographs and these crystalline layers contribute for slightly better mechanical properties than mLDHs. For further understanding on the reinforcing capabilities of mLDHc, study on improvements on mechanical properties toward higher loading of mLDHc was performed. From Table III marginal increases in the tensile strength as well as elongation at break are observed, but the enhancements in mechanical properties (with respect to the amount of filler) are limited. Nanocomposites with higher loading of mLDHc shows slightly better tensile strength and higher elongations at break indicating that the stearate groups surely act as internal lubricants. Higher concentrations of mLDHc correspond to higher amounts of stearate groups inside the nanocomposite and they facilitate chain slippage and encourage higher elongation at break by limiting the mechanical strength of the nanocomposite. For comparison, the molar concentration of zinc and stearate ions in mLDHs is calculated and a correspondingly equivalent composite containing ZnO and stearic acid (added separately) is considered as the reference compound. Nevertheless, even at least concentration of 5 phr, LDH outperforms ZnO filled systems and this is surely a superiority of using LDH.

Dynamic mechanical thermal analysis is performed to understand the filler–polymer interaction as well as filler–filler interaction by temperature sweep and strain sweep mode and their respective diagrams are given in Figure 5. The temperature sweep experiment, Figure 5(a), reveals a marginal negative shift and noticeable reduction in tan δ peak for mLDHc. The temperature corresponding to the maximum peak height represents the glass transition temperature (T_g) of the material. Apparently, mLDHc composite exhibits almost 4°C lower T_g values as compared to uLDHc and mLDHs composites. Also, for the better understanding of the filler–polymer interaction, storage modulus (E') is plotted against temperature, but there is hardly any considerable change in storage moduli. From the above

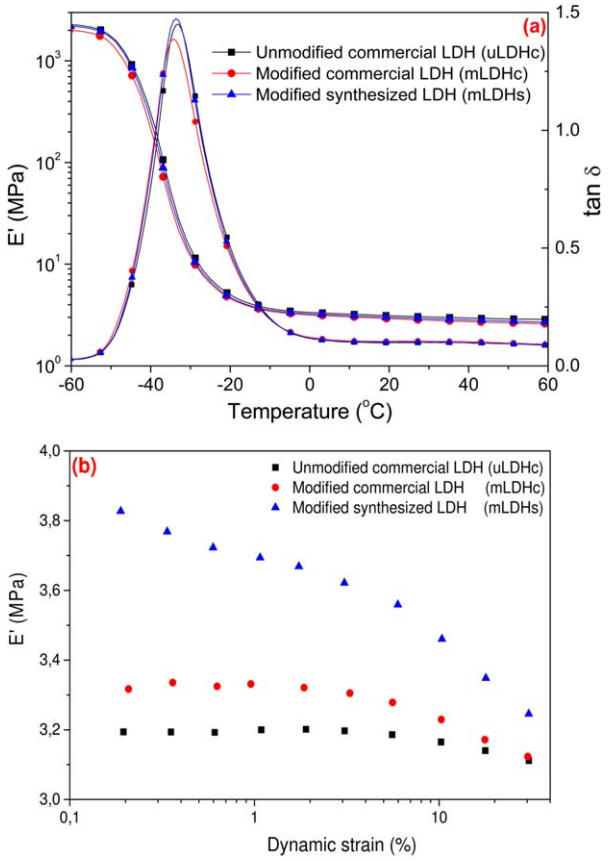

Figure 5. (a) Temperature sweep curves and (b) amplitude sweep curves for NBR 1846 with different LDH. [Color figure can be viewed in the online issue, which is available at wileyonlinelibrary.com.]

Table III. Stress–Strain and Hardness Data for NBR 1846 with 5 phr of Different LDH and Increasing mLDHc Content

	Stress (MPa)						
	50%	100%	200%	300%	Tensile strength (MPa)	Elongation at break (%)	Hardness (Shore A)
ZnO. Eq	0.7	0.9	1.1	1.3	1.7	411	45
5 uLDHc	0.7	1.0	1.6	2.4	4.7	495	48
5 mLDHs	0.7	0.9	1.3	1.6	2.4	447	46
5 mLDHc	0.7	1.0	1.3	1.7	2.6	466	47
10 mLDHc	0.7	1.0	1.4	1.9	3.7	522	48
15 mLDHc	0.7	1.1	1.5	2	3.4	492	49
50 mLDHc	1.0	1.2	1.4	1.7	5.3	687	56

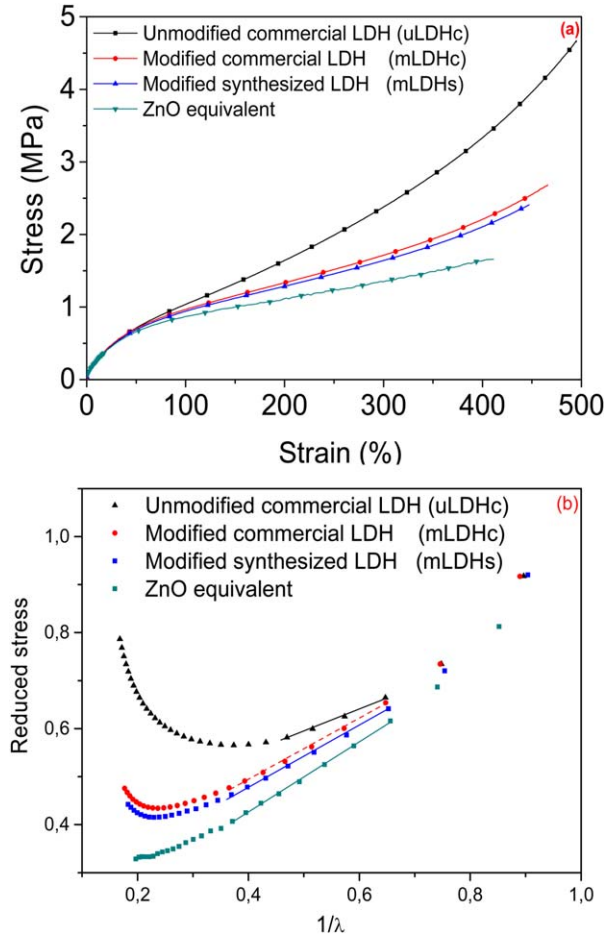

Figure 6. (a) Stress–strain plot and (b) Mooney–Rivlin plot for NBR 1846 unconditioned samples with different LDH. [Color figure can be viewed in the online issue, which is available at wileyonlinelibrary.com.]

discussions it can be concluded that mLDHc based nanocomposites show a better filler–polymer interaction than uLDHc and mLDHs composites due to the reduction in the tan δ peak height. Figure 5(b) shows the amplitude sweep experiment conducted in an attempt to understand the presence of any local filler–filler associations or clustering like Payne effect.[34,35] In this case, the amount of incorporated filler is very less and the possibilities of obtaining a percolated filler–filler network inside the soft rubber matrix are very less, yet a dependence of storage modulus with respect to strain was observed. In reference to the plot it can be noted that mLDHs possesses a higher filler–filler interaction when compared to the other nanocomposites.

The crosslink density values obtained by equilibrium swelling method are given in Table IV. From the table it can be noted that there is a reduction in crosslink density, in accordance to the stearate modification. This holds true for pre-swollen as well as for fresh samples, additionally the fresh samples have lower crosslink density values than pre-swollen samples. The reason for the higher crosslink density exhibited by the pre-swollen samples could be due to increase in chain entanglements which occurred when the sample was allowed to swell and de-swell. From the TGA estimations, it is understood that the amount of stearate content in the LDH is in the order mLDHs > mLDHc > uLDHc, accordingly the crosslink densities adhere to the same order which in turn signifies its dependence on the amount of stearate modification.

The Mooney–Rivlin equation is one of the widely used techniques for the evaluation of the degree of crosslinking for the elastomers[36–39] and is governed by the phenomenological theory of rubber elasticity.[21,31,40,41] The crosslink density values obtained by Mooney–Rivlin theory are also listed in Table IV. The stress–strain plot and the Mooney–Rivlin plot for the unconditioned samples are shown in Figure 6, it is clear that stearic acid modification in LDH hampers the mechanical properties in comparison to uLDHc composites. Similar effect was observed in Mooney–Rivlin plot, implying the reduction in reduced stress values by the effective stearate modification. However the reduced stress of all LDH based vulcanizates are higher compared to zinc oxide cured vulcanizates. This substantiates LDH as an alternative material to cure the NBR matrix as well as offer some reinforcement. Moreover in the high elongation regions, the Mooney–Rivlin graphs turns upward for all LDH based composites except zinc oxide cured vulcanizates and this distinctly explains that the layered morphology of LDH contributing to the mechanical reinforcement of NBR. The Mooney–Rivlin plots for the modified LDH nanocomposites are mostly linear in the region $\lambda = 0.4$ to 0.6 but uLDHc nanocomposite displays a curve rather than a straight line and it is difficult to make a reliable

Table IV. Crosslink Density Values Obtained for Different LDH by Various Methods

	Equilibrium swelling method		Mooney–Rivlin theory			
	Conditioning	CLD (mol/cc)	Slope	Intercept	Conditioning	CLD (mol/cc)
uLDHc	Pre-swollen samples	13.21×10^{-5}	0.181	0.165	Subjected to hysteresis	6.68×10^{-5}
mLDHc		10.83×10^{-5}	0.153	0.146		5.89×10^{-5}
mLDHs		9.86×10^{-5}	0.158	0.143		5.77×10^{-5}
uLDHc	Fresh samples	9.20×10^{-5}	0.166	0.213	Fresh samples	8.61×10^{-5}
mLDHc		7.87×10^{-5}	0.272	0.139		5.65×10^{-5}
mLDHs		7.83×10^{-5}	0.279	0.129		5.21×10^{-5}
ZnO eq.		4.81×10^{-5}	0.330	0.082		3.32×10^{-5}

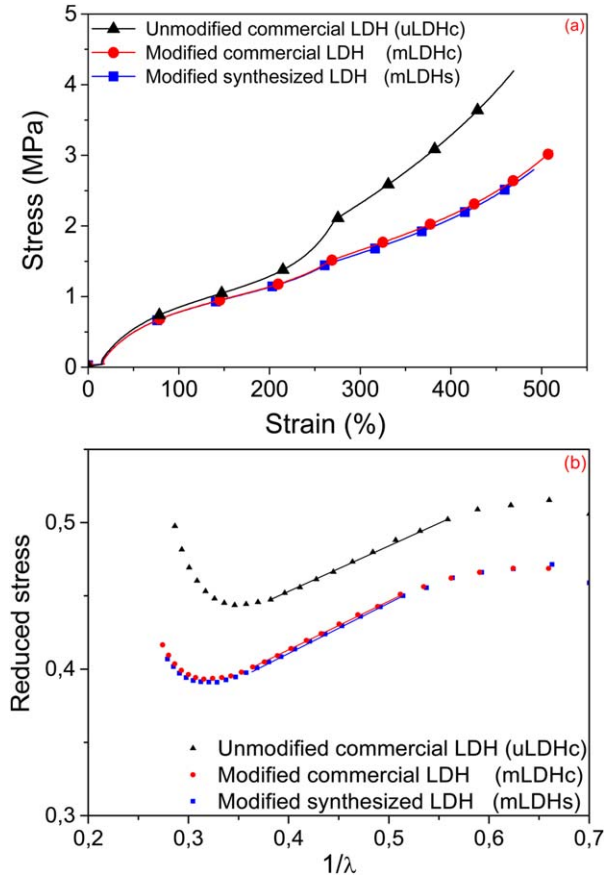

Figure 7. (a) Stress–strain plot and (b) Mooney–Rivlin plot for NBR 1846 preconditioned samples with different LDH. [Color figure can be viewed in the online issue, which is available at wileyonlinelibrary.com.]

linear fit for the curve to obtain the slope and the intercept. Concurrently, it was discussed earlier that the cured compounds show a "Payne like effect" due to a local filler–filler network, hence in order to destroy this local network, the samples were subjected to 10 times cyclic deformation and the stress–strain and Mooney–Rivlin plots were redrawn and depicted in Figure 7. Figure 7(a) shows the stress–strain plot for stretched nanocomposites which tend to follow two different patterns, the first region (below 300% strain) of the plot corresponds to the broken local filler network, disturbance of the chain conformation, Mullins effect, and other minor effects. The second region (above 300% strain) of the plot corresponds to the unstrained undisturbed regions and they follow the path similar to that of unstretched nanocomposites. The Mooney–Rivlin plot is now considered only till the strain where the deviation occurs. Figure 7(b) represent the Mooney–Rivlin plots of prestretched samples and the plots of the nanocomposites remain parallel differing in their intercept values representing different crosslink densities. Here also it was noticed that the crosslinking efficiency of uLDHc is higher as compared to both of the stearic acid modified LDH nanocomposites. The crosslink density values correlate with the solvent swelling values, and the crosslinking density values of the unstretched samples are higher than the prestretched samples. This is because of the high entanglement density and also the filler–filler networks are broken during hysteresis, whereas the crosslink density values of the prestretched samples depends mostly on the actual crosslinks present in the network excluding certain chain entanglements, etc. For reference studies, fresh ZnO equivalent sample is represented, and LDH filled systems prove to be far superior in terms of the crosslink density of the nanocomposites.

CONCLUSIONS

This study was carried out in an effort to understand the behavior and highlight the advantages and disadvantages of stearate modification in Zn-Al-LDH. Rheometric studies indicated that stearate modification of LDH played an important role in improving the scorch safety, cure rate, and decreasing the optimum cure time. XRD results indicated that intercalation was successful in LDH by stearic acid modification; despite it had adverse effects on the mechanical properties and crosslinking density of NBR. Nevertheless, all LDH based nanocomposites showed better mechanical properties and a higher crosslinking density compared to ZnO cured vulcanizates.

Utilization of LDH as nanosized fillers may not offer a huge reinforcement effect (when compared to carbon or silica-based systems) by virtue of its mineral layered structure, however highest reinforcement was realized for unmodified LDH nanocomposite. In contrast, if stearic acid modified LDH are used, there are possibilities of the crystalline structure of the LDH getting collapsed during the course of vulcanization reaction. The most plausible explanation therefore would be the participation of zinc and stearate ions in the vulcanization reaction, which combine with sulfur and organic accelerators to form a soluble sulfurating complex and this is an *in situ* sulfur crosslinking precursor at vulcanizing condition.

ACKNOWLEDGMENTS

Eshwaran is thankful to DAAD for the financial support and sincerely thank Mrs. Uta Reuter, Mrs. Sabine Krause, and Mr. Holger Scheibner for their valuable support and contributions in this work.

REFERENCES

1. Rooj, S.; Das, A.; Stockelhuber, K. W.; Wang, D. Y.; Galiatsatos, V.; Heinrich, G. *Soft Matter* **2013**, *9*, 3798.
2. Raman, V. S.; Rooj, S.; Das, A.; Stöckelhuber, K. W.; Simon, F.; Nando, G. B.; Heinrich, G. *J. Macromol. Sci. A* **2013**, *50*, 1091.
3. Das, A.; Wang, D.-Y.; Leuteritz, A.; Subramaniam, K.; Greenwell, H. C.; Wagenknecht, U.; Heinrich, G. *J. Mater. Chem.* **2011**, *21*, 7194.
4. Leuteritz, A.; Kutlu, B.; Meinl, J.; Wang, D.; Das, A.; Wagenknecht, U.; Heinrich, G. *Mol. Cryst. Liq. Cryst.* **2012**, *556*, 107.
5. Heideman, G.; Noordermeer, J. W. M.; Datta, R. N.; van Baarle, B. *Rubber Chem. Technol.* **2004**, *77*, 336.
6. Fosmire, G. J. *Am. J. Clin. Nutr.* **1990**, *51*, 225.
7. Loadman, J. Tears of the Tree: The Story of Rubber—A Modern Marvel; OUP: Oxford, **2005**.

8. Chapman, A. V. *Safe Rubber Chemicals: Reduction of zinc levels in rubber compounds*, **1997**, TARRC/MRPRA, 20.
9. Heideman, G.; Noordermeer, J. W. M.; Datta, R. N.; van Baarle, B. *Rubber Chem. Technol.* **2005**, *78*, 245.
10. Heideman, G.; Noordermeer, J. W. M.; Datta, R. N.; van Baarle, B. *Rubber Chem. Technol.* **2006**, *79*, 561.
11. Das, A.; George, J. J.; Kutlu, B.; Leuteritz, A.; Wang, D. Y.; Rooj, S.; Jurk, R.; Rajeshbabu, R.; Stockelhuber, K. W.; Galiatsatos, V.; Heinrich, G. *Macromol. Rapid Commun.* **2012**, *33*, 337.
12. Kuila, T.; Acharya, H.; Srivastava, S. K.; Bhowmick, A. K. *J. Appl. Polym. Sci.* **2007**, *104*, 1845.
13. Kotal, M.; Kuila, T.; Srivastava, S. K.; Bhowmick, A. K. *J. Appl. Polym. Sci.* **2009**, *114*, 2691.
14. Depan, D.; Singh, R. P. *J. Appl. Polym. Sci.* **2010**, *115*, 3636.
15. Pradhan, B.; Srivastava, S. K.; Ananthakrishnan, R.; Saxena, A. *J. Appl. Polym. Sci.* **2011**, *119*, 343.
16. Feng, J.; Liao, Z.; Zhu, J.; Su, S. *J. Appl. Polym. Sci.* **2013**, *127*, 3310.
17. Rives, V. Layered Double Hydroxides: Present and Future; Nova Science Publishers: Hauppage, NY, **2001**.
18. Mahboobeh, E.; Yunus, W. M. Z. W.; Hussein, Z.; Ahmad, M.; Ibrahim, N. A. *J. Appl. Polym. Sci.* **2010**, *118*, 1077.
19. Evans, D. G.; Duan, X. *Chem. Commun.* **2006**, 485.
20. Basu, D.; Das, A.; Stockelhuber, K. W.; Wagenknecht, U.; Heinrich, G. *Prog. Polym. Sci.* **2014**, *39*, 594.
21. Pradhan, S.; Costa, F. R.; Wagenknecht, U.; Jehnichen, D.; Bhowmick, A. K.; Heinrich, G. *Eur. Polym. J.* **2008**, *44*, 3122.
22. Williams, G. R.; O'Hare, D. *J. Mater. Chem.* **2006**, *16*, 3065.
23. Omnès, B.; Thuillier, S.; Pilvin, P.; Grohens, Y.; Gillet, S. *Compos. A* **2008**, *39*, 1141.
24. Chen, G. *J. Appl. Polym. Sci.* **2007**, *106*, 817.
25. Eshwaran, S. B.; Basu, D.; Kutlu, B.; Leuteritz, A.; Wagenknecht, U.; Stöckelhuber, K. W.; Naskar, K.; Das, A.; Heinrich, G. *Polym. Plast. Technol. Eng.* **2014**, *53*, 65.
26. Heideman, G.; Datta, R. N.; Noordermeer, J. W. M.; Baarle, B. v. *J. Appl. Polym. Sci.* **2005**, *95*, 1388.
27. Oh, J.-M.; Park, C.-B.; Choy, J.-H. *J. Nanosci. Nanotechnol.* **2011**, *11*, 1632.
28. Zammarano, M.; Franceschi, M.; Bellayer, S.; Gilman, J. W.; Meriani, S. *Polymer* **2005**, *46*, 9314.
29. Flory, P. J.; Rehner, J. *J. Chem. Phys.* **1943**, *11*, 521.
30. Hwang, W.-G.; Wei, K.-H.; Wu, C.-M. *Polym. Eng. Sci.* **2004**, *44*, 2117.
31. Furukawa, J.; Onouchi, Y.; Inagaki, S.; Okamoto, H. *Polym. Bull.* **1982**, *6*, 381.
32. Costa, F. R.; Saphiannikova, M.; Wagenknecht, U.; Heinrich, G. *Adv. Polym. Sci.* **2008**, *210*, 101.
33. Chukwu, M. N.; Madufor, I. C.; Ayo, M. D.; Ekebafe, L. O. *Pac. J. Sci. Technol.* **2011**, *12*, 7.
34. Payne, A. R. *J. Appl. Polym. Sci.* **1962**, *6*, 57.
35. Payne, A. R.; Whittaker, R. E. *Rubber Chem. Technol.* **1971**, *44*, 440.
36. Mark, J. E. *Rubber Chem. Technol.* **1982**, *55*, 762.
37. Morris, M. C. *J. Appl. Polym. Sci.* **1964**, *8*, 545.
38. Spathis, G. D. *J. Appl. Polym. Sci.* **1991**, *43*, 613.
39. Sekkar, V.; Narayanaswamy, K.; Scariah, K. J.; Nair, P. R.; Sastri, K. S.; Ang, H. G. *J. Appl. Polym. Sci.* **2007**, *103*, 3129.
40. Hagen, R.; Salmén, L.; Stenberg, B. *J. Polym. Sci. Part B: Polym. Phys.* **1996**, *34*, 1997.
41. Roberts, A. D. Natural Rubber Science and Technology; Oxford University Press: Oxford, UK, **1988**.